Drug Design, Development and Therapy

Dovepress
open access to scientific and medical research

Open Access Full Text Article

ORIGINAL RESEARCH

Mechanistic Study of *Schisandra chinensis* Fruit Mixture Based on Network Pharmacology, Molecular Docking and Experimental Validation to Improve the Inflammatory Response of DKD Through AGEs/RAGE Signaling Pathway

Hongdian Li[1,*], Ao Dong[1,*], Na Li[1], Yu Ma[1], Sai Zhang[1], Yuanyuan Deng[1], Shu Chen[1], Mianzhi Zhang[1,2]

[1]Department of Nephrology, Dongfang Hospital of Beijing University of Chinese Medicine, Beijing, People's Republic of China; [2]Department of Nephrology, Tianjin Academy of Traditional Chinese Medicine Affiliated Hospital, Tianjin, People's Republic of China

*These authors contributed equally to this work

Correspondence: Mianzhi Zhang, Email zhangmianzhi@vip.sina.com

Background: Diabetic kidney disease (DKD) is a major cause of end-stage renal disease (ESRD), and inflammation is the main causative mechanism. *Schisandra chinensis* fruit Mixture (SM) is an herbal formulation that has been used for a long time to treat DKD. However, its pharmacological and molecular mechanisms have not been clearly elucidated. The aim of this study was to investigate the potential mechanisms of SM for the treatment of DKD through network pharmacology, molecular docking and experimental validation.

Methods: The chemical components in SM were comprehensively identified and collected using liquid chromatography-tandem mass spectrometry (LC-MS) and database mining. The mechanisms were investigated using a network pharmacology, including obtaining SM-DKD intersection targets, completing protein–protein interactions (PPI) by Cytoscape to obtain key potential targets, and then revealing potential mechanisms of SM for DKD by GO and KEGG pathway enrichment analysis. The important pathways and phenotypes screened by the network analysis were validated experimentally in vivo. Finally, the core active ingredients were screened by molecular docking.

Results: A total of 53 active ingredients of SM were retrieved by database and LC-MS, and 143 common targets of DKD and SM were identified; KEGG and PPI showed that SM most likely exerted anti-DKD effects by regulating the expression of AGEs/RAGE signaling pathway-related inflammatory factors. In addition, our experimental validation results showed that SM improved renal function and pathological changes in DKD rats, down-regulated AGEs/RAGE signaling pathway, and further down-regulated the expression of TNF-α, IL-1β, IL-6, and up-regulated IL-10. Molecular docking confirmed the tight binding properties between (+)-aristolone, a core component of SM, and key targets.

Conclusion: This study reveals that SM improves the inflammatory response of DKD through AGEs/RAGE signaling pathway, thus providing a novel idea for the clinical treatment of DKD.

Keywords: *Schisandra chinensis* fruit mixture, diabetic kidney disease, traditional Chinese medicine, network pharmacology, molecular docking

Introduction

Diabetic kidney disease (DKD) is one of the most serious and common microvascular complications of diabetes and is currently the leading cause of end-stage renal disease (ESRD). According to a comprehensive summary of epidemiological data, diabetes, hypertension or the cumulative effect of both are responsible for 80% of ESRD formation and

Received: 26 November 2022
Accepted: 20 February 2023
Published: 27 February 2023

diabetic patients are 10 times more likely to develop ESRD than non-diabetic population.[1] The prevalence of DKD is increasing in a violent trend with the expansion of the diabetes population. There are currently about 537 million people with diabetes worldwide, and it is expected to increase to 783 million by 2045, of which 30–40% will develop DKD.[2] Patients with ESRD require long-term dialysis or kidney transplantation, which seriously affects their quality of life and survival time, while greatly increasing the socioeconomic burden.[3]

The current treatment strategy for DKD is based on symptomatic supportive therapy with strict control of blood glucose and blood pressure levels; however, there are bottlenecks in efficacy. For example, angiotensin-converting enzyme inhibitors and angiotensin receptor antagonist drugs are effective in reducing proteinuria, but hardly prevent the development of renal fibrosis.[4–7] Sodium-glucose-linked transporter-2 inhibitors have been considered in recent years as the most promising new drugs for the treatment of DKD,[8] which control glycemia and diabetes-related complications by inhibiting renal reabsorption of glucose, lowering the renal tissue glucose threshold, and promoting urinary glucose excretion. However, the current evidence from clinical studies is not sufficient. In addition, a recent study has shown that dapagliflozin increases the economic burden of kidney disease treatment in the United States.[9] For these reasons, there is an urgent need to find cost-effective ways to delay the progression of DKD.[10,11]

Traditional Chinese Medicine (TCM) has been used to treat kidney disease for thousands of years. In China and some other Asian countries, TCM has been found to be effective in the treatment of DKD.[12–14] Our previous meta-analysis based on 2105 DKD patients demonstrated that TCM combined with Western medicine significantly reduced renal damage indicators and blood glucose levels and had the same safety as conventional Western therapy.[15] Schisandra chinensis fruit Mixture (SM) is a Chinese herbal formula for DKD that consists of three herbs: *Schisandra chinensis fruit* ("Wuweizi" in Chinese, WWZ), *Rhizoma chuanxiong* ("Chuanxiong" in Chinese, CX) and *Oyster shells* ("Muli" in Chinese, ML). Our previous study showed that WWZ alcohol extract was effective in preventing DKD-induced EMT[16] and demonstrated that SM may treat DKD via the PI3K/AKT pathway,[17] but the exact mechanism remains to be further investigated. This is mainly due to the multi-component, multi-target and multi-pathway therapeutic characteristics of herbal formulas.

Network pharmacology emphasizes on improving the therapeutic effect of drugs and reducing toxic side effects through multi-path modulation, thus improving the success rate of clinical trials of new drugs and saving drug development costs. In recent years, network pharmacology has been receiving attention as a bridge between TCM and modern medicine.[18,19] Molecular docking is a method for drug design by the characteristics of the receptor and the mode of interaction between the receptor and the drug molecule and has been used in recent years as an adjunct to drug research together with network pharmacology.[20]

Notably, this study is a novel experiment that uses a combination of systems biology, computer technology and experimental validation to combine TCM theory with new modern medical technology to investigate in depth the efficacy and mechanism of action of SM on DKD. This is a new type of research approach that is gaining popularity (see Figure 1 for the system workflow).

Methods and Materials

Collection of SM Potential Active Ingredients and Related Targets

The potential chemical composition of three herbs in SM was obtained from the website of Chinese herbal ingredients online. Because these sites are updated at different rates and with different emphases, the composition and genetic targets of the same herbal medicine are not consistent across databases. For example, the Traditional Chinese Medicine Systems Pharmacology Database and Analysis Platform (TCMSP),[21] the most commonly used database in network pharmacology and is the only database that provides oral bioavailability (OB) and drug-likeness (DL), but the database only contains nearly 500 herbs. Traditional Chinese Medicine integrative database (TCMID)[22] records the largest variety of herbs among all databases (containing 8159 herbs); however, it records limited information on herb targets. The Encyclopedia of Traditional Chinese Medicine (ETCM)[23] includes standardized information on commonly used herbal medicines, however it only collects 402 herbs. A Bioinformatics Analysis Tool for Molecular mechanism of Traditional Chinese Medicine (BATMAN-TCM) database,[24] although not comprehensive in recording herbs, has very comprehensive

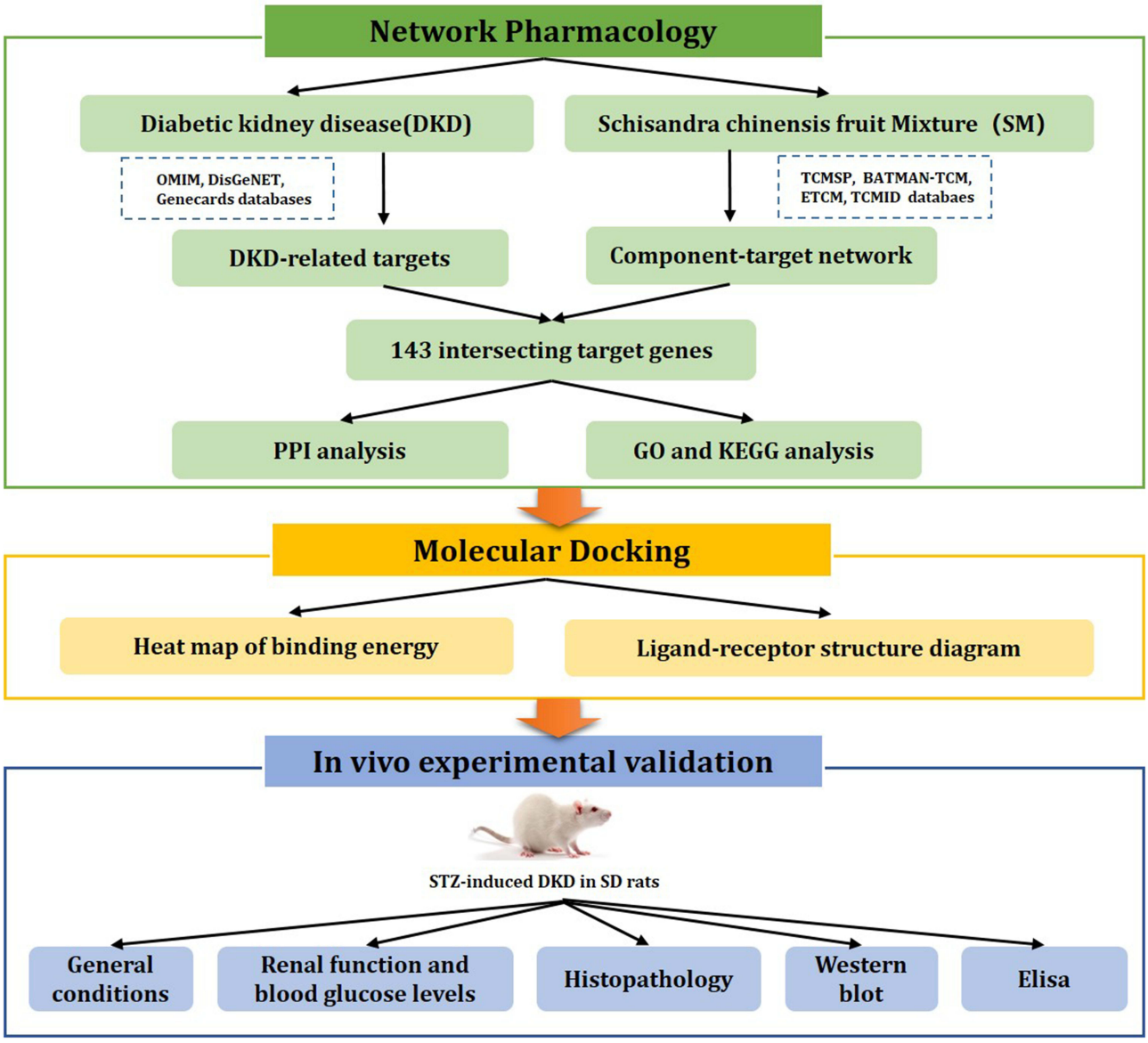

Figure 1 Main workflow of this study.

information on chemical composition-related targets, and only provides a relatively small number of herbal components. The above four databases are the most widely used databases for herbal and chemical composition information. Based on the characteristics of these databases, we optimized the search strategy in order to expect comprehensive and accurate information on drug components and related targets.

We used OB ≥ 30% and DL ≥ 0.18 as screening conditions in TCMSP for initial screening of drug ingredients. DL is a qualitative concept used in drug design for an estimate on how "drug-like" a prospective compound is, which helps to optimize pharmacokinetic and pharmaceutical properties, such as solubility and chemical stability.[25] OB indicates the percentage of an oral dose of unchanged drug that reaches the body's circulation, and a high OB is often a key indicator for determining the properties of a biologically active molecule as a therapeutic agent.[26] Ingredients not recorded in TCMSP were screened using the SwissADME database for favorable gastrointestinal absorption and high DL values.[27] In addition, we found that certain ingredients, although not meeting the conditions of OB < 30% and DL < 0.18, have broad pharmacological activity or are known to be major components in SM (such as Ligustrazine,[28] Retinol,[29] etc.) and therefore should also be added as potential active ingredients in SM. The TCMSP database, the BATMAN database and

Swiss Target Prediction[30] were collectively used as potential targets for predicting components, and the names of relevant targets were standardized through the UniProt database.[31]

Access to Drug-Disease Intersecting Targets

The human disease gene databases Genecards (http://www.genecards.org/), OMIM (https://omim.org/) and Disgenet (https://www.disgenet.org/) were searched using "diabetic kidney disease" and "diabetic nephropathy" as search terms, respectively. Scores greater than 10 and 0.1 were selected from the Genecards database and the Disgenet database, respectively. All obtained disease targets were combined to remove duplicate values to obtain the complete DKD-related targets. In addition, we used the Venn 2.1.0 platform to obtain the SM-DKD intersection targets.

PPI and Core Network Construction

The cross-targets of SM and DKD were uploaded to the STRING online database platform, and the PPI network maps of the cross-targets were obtained by setting the organism as "Homo sapiens". The obtained information was then uploaded to Cytoscape 3.7.2 software to filter and refine the core network based on Degree, Betweenness and Closeness, and parameters were calculated with the help of Centiscape plug-in to form a complete PPI protein interaction map.

GO Analysis and KEGG Pathway Analysis

GO and KEGG pathway enrichment analysis of bioactive targets was performed by DAVID 6.8 platform. The top 20 significantly enriched biological properties and the 20 significantly enriched pathways were visualized by SM for DKD. KEGG and GO images were plotted using the bioinformatics online website (http://www.bioinformatics.com.cn/).

Molecular Docking Verification

The 3D structure of the protein was obtained from the RCSB PDB database,[32] and the ingredient was obtained from the PubChem database.[33] Molecular docking validation of the active ingredient and key targets of the herb was performed using AutoDockTools (v1.5.7)[34] and PyMOL (v 2.3.0).[35]

Experimental Animals

Thirty adult male Sprague-Dawley rats (weighing 180–220 g, 6 weeks old) were purchased from Beijing Vital River Laboratory Animal Technology Co., Ltd. All rats were housed at a temperature of (22±2)°C, relative humidity (60±10)%, and kept in a rat house with 12h light/12h dark alternation, and were fed with the same free water and feed. The study was conducted under the National Guidelines for ethical review of the welfare of laboratory animals (GB/T35892-2018) and was approved by the Animal Experimentation Ethics Committee of the Dongfang Hospital, Beijing University of Chinese Medicine (ethical approval number: DFYY202102R).

Interventional Drug Use

SM consisted of WWZ, CX and ML in the ratio of 3:2:1. The mixed herbs were macerated in 8 times the volume of ethanol (90%, v/v), heated and refluxed twice in 6 times the volume of ethanol (90%, v/v), the two extracts were combined, left to filter, and concentrated into an infusion by recovering ethanol under reduced pressure and stored at 4°C.

Liquid Chromatography-Tandem Mass Spectrometry (LC-MS)

Schisandrin B, schisandrin A, schisandrol A, schisantherin A, betaine, ferulic acid, tetramethylpyrazine and senkyunolide A were purchased from Shanghai Jiuzhi Chemicals Co., Ltd. (Shanghai, China), and the mass fractions of the controls were all greater than 99%. LC/MS grade acetonitrile and HPLC grade methanol were purchased from Merck, Germany, and formic acid (chromatographic alcohol) was purchased from CNW. All other reagents were analytically pure. The water used for the experiment was Watson's distilled water. Preparation of the control solution: take appropriate amount of schisandrin B, schisandrin A, schisandrol A, schisantherin A, betaine, ferulic acid, tetramethylpyrazine and senkyunolide A, and add methanol to prepare a mixed control solution with mass concentration of 1mg/mL, filter through 0.22μm microporous membrane for LC/MS detection and analysis. SM consisted of WWZ, CX and ML in the ratio of

3:2:1. The mixed herbs were macerated in 8 times the volume of ethanol (90%, v/v), heated and refluxed twice in 6 times the volume of ethanol (90%, v/v), the two extracts were combined, left to filter, and concentrated into an infusion by recovering ethanol under reduced pressure and stored at 4°C. The SM was diluted with methanol to a concentration of 0.1 g/mL, aspirated about 1 mL of liquid sample, centrifuged at 10000 rpm for 10 min and then aspirated 100 μL of supernatant, added 400 μL (methanol:acetonitrile = 1:1) of precipitant to precipitate the impurities, centrifuged at 10000 rpm for 10 min and then 100 μL was taken for LC-MS analysis. The LC-MS analysis of the samples was performed on a DIONEX Ultimate 3000 (Dionex, USA). The separation was performed on an ACQUITY BEH C18 (2.1 mm × 50 mm, 1.7 μm) column at 40 °C with a flow rate of 0.25 mL/min and an injection volume of 5 μL. The mobile phase A was water (containing 2 mmoL/L ammonium formate and 0.1% formic acid) and B was acetonitrile, and the gradient elution procedure is shown in Table 1.

Induction of DKD and Drug Administration

Thirty male SD rats were randomly grouped, including 6 rats in the control group and 24 rats in the DKD group. Twenty-four rats in the DKD group were fed with high-sugar and high-fat (HSHF) diet (Beijing Keao Xieli Feed Co., Ltd., China) for 6 weeks, and streptozotocin (STZ) 35 mg/kg was injected intraperitoneally to construct a type 2 diabetic nephropathy model. Random blood glucose was measured for 3 consecutive days after 72h of STZ injection. Twenty-four-hour urine protein quantification (24hUTP) was collected 2 weeks after STZ injection. HSHF feeds were continued during this period.[36] The whole modeling cycle was 8 weeks. Random blood glucose ≥16.7 mmol/L and 24hUTP ≥30 mg/24h were used as the criteria for successful modeling.

The rats with successful modeling were then divided into 4 groups of 6 rats each by randomized control method: DKD group, low-dose group (SM-L), medium-dose group (SM-M) and high-dose group (SM-H). SM dose groups were given different doses of SM by gavage (SM-L: 1.5g/kg/d; SM-M: 3g/kg/d; SM-H; 6g/kg/d), and the medium dose of animals was converted by calculating the surface area ratio between experimental animals and humans. The low dose was 1/2 of the medium dose and the high dose was 2 times of the medium dose. Equal volumes of deionized water were given simultaneously to the DKD and control groups by gavage once daily for 12 weeks.

Sample Collection

Blood glucose, water intake and food intake were measured, and urine was collected from each rat in separate metabolic cages to determine 24hUTP. Twelve weeks later, blood was collected from the abdominal aorta, both kidneys were excised, fat and perirenal membranes were removed, fixed in 4% paraformaldehyde for 48 h, then dewaxed, embedded and sectioned. The remaining kidney tissues were cut into small pieces and placed in −80°C refrigerator for Western blot.

24hUTP, Serum Creatinine and Blood Urea Nitrogen (BUN)

After 12 weeks of dosing, 24-hour urine was collected from rats, and the urine was centrifuged at 3000 rpm for 10 minutes, and the 24hUTP was measured by a urine protein kit (Nanjing Jiancheng, China). The collected blood samples were centrifuged at 4°C for 15 minutes at low speed (3000 rpm), and the supernatant was aspirated and stored at −80°C

Table 1 Gradient Conditions

Time (min)	A (%)	B (%)
0	95	5
2.00	95	5
42.00	5	95
47.00	5	95
47.10	95	5
50.00	95	5

Notes: A: distilled water containing 2 mmoL/L ammonium formate and 0.1% formic acid; B: acetonitrile.

in the refrigerator. The blood samples were thawed on ice when needed for testing, and then creatinine and BUN levels were measured in rats using specialized kits (Nanjing Jiancheng, China).

Pathological Histology

The upper segment of each kidney was fixed in 4% formaldehyde, rinsed with running water, routinely dehydrated, transparent, dipped in wax, embedded, sectioned, and dewaxed. Staining was performed according to hematoxylin-eosin (HE) kit, periodic acid-silver methenamine (PASM) kit, and MASSON (Zhongshan Jinqiao, China) kit, and the stained sections were dehydrated and preserved with neutral gum seal. Observations were made under light microscopy and photographed. Renal tissues fixed in 2.5% glutaraldehyde were subjected to ultrathin tissue sections and observed by transmission electron microscopy (TEM). We used ImageJ software to evaluate MASSON stained tissue images and to estimate the area of fibrosis. For each rat, images were evaluated at 40x magnification in 3 different fields of view.

Enzyme Linked Immunosorbent Assay (ELISA)

Inflammation-associated factors were detected by ELISA. Briefly, kidney tissues were washed and crushed, homogenized in phosphate buffer, and the supernatant was centrifuged according to standards and then taken for the assay. The kit was purchased from Shanghai Enzyme-linked Biotechnology Co. The operator is required to strictly follow the instructions.

Western Blot

Kidney tissues of the same size were put into EP tubes, and RIPA lysate and small steel beads were added and put into a high-throughput tissue grinder for grinding. After standing on ice for one hour, the tissues were centrifuged. The supernatant was removed into a new EP tube for BCA protein quantification and placed in a constant temperature metal bath to denature the protein. Prepare 10% SDS-PAGE gels, and after loading, electrophoresis at 110V for 2h, transferring the membrane at 100V for 2h, and 5% milk closure, cut the membrane, add AGEs and RAGE primary antibodies obtained from dilution, and incubate at 4°C overnight; after washing the film with TBST, the secondary antibody corresponding to the source of the primary antibody was added and shaken slowly at room temperature for one hour, then washed again with TBST, color development was performed with ECL western blotting substrate (Solarbio, China), and the chemiluminescent imager was exposed. Image J was used for grayscale analysis. The results were expressed as the relative expression of the target protein to GAPDH.

Statistical Method

All measures were expressed as mean ± standard error (x±s), and data were analyzed using SPSS 22.0 (SPSS for Windows, Chicago, SPSS Inc.) statistical software and graphs were prepared using Graph Pad Prism 8.0 software. One-way ANOVA was used for comparison between groups, and differences were considered statistically significant at $P<0.05$ or $P<0.01$.

Results

Screening of the Main Active Ingredients in SM

The active ingredients in SM, including schisandrin B, schisandrin A, schisandrol A, schisantherin A, betaine, ferulic acid, tetramethylpyrazine and senkyunolide A, were analyzed by LC/MS (Figure 2). By searching the TCMSP, BATMAN-TCM, ETCM, TCMID databases and related literature, 46 potential active ingredients were obtained in SM. The numbers of potential active ingredients in WWZ, CX and ML were 20, 22 and 6, respectively, among which Spathulenol and Dibutyl Phthalate were common to CX and WWZ. Combining the results of the LC/MS and database, we finally included 53 chemical components into the later study. We recorded the "Molecule ID" of these components to make it easier for the reader to look them up (we used the PubChem CID as the Molecule ID of these components). Most of these chemical ingredients had good OB and DL, and those ingredients that did not meet OB ≥ 30% and DL ≥ 0.18 had good biological activity or were major components, so we included them (Table 2). A search of the TCMSP, BATMAN and Swiss Target Prediction databases yielded 592, 596 and 134 targets for WWZ, CX and ML active

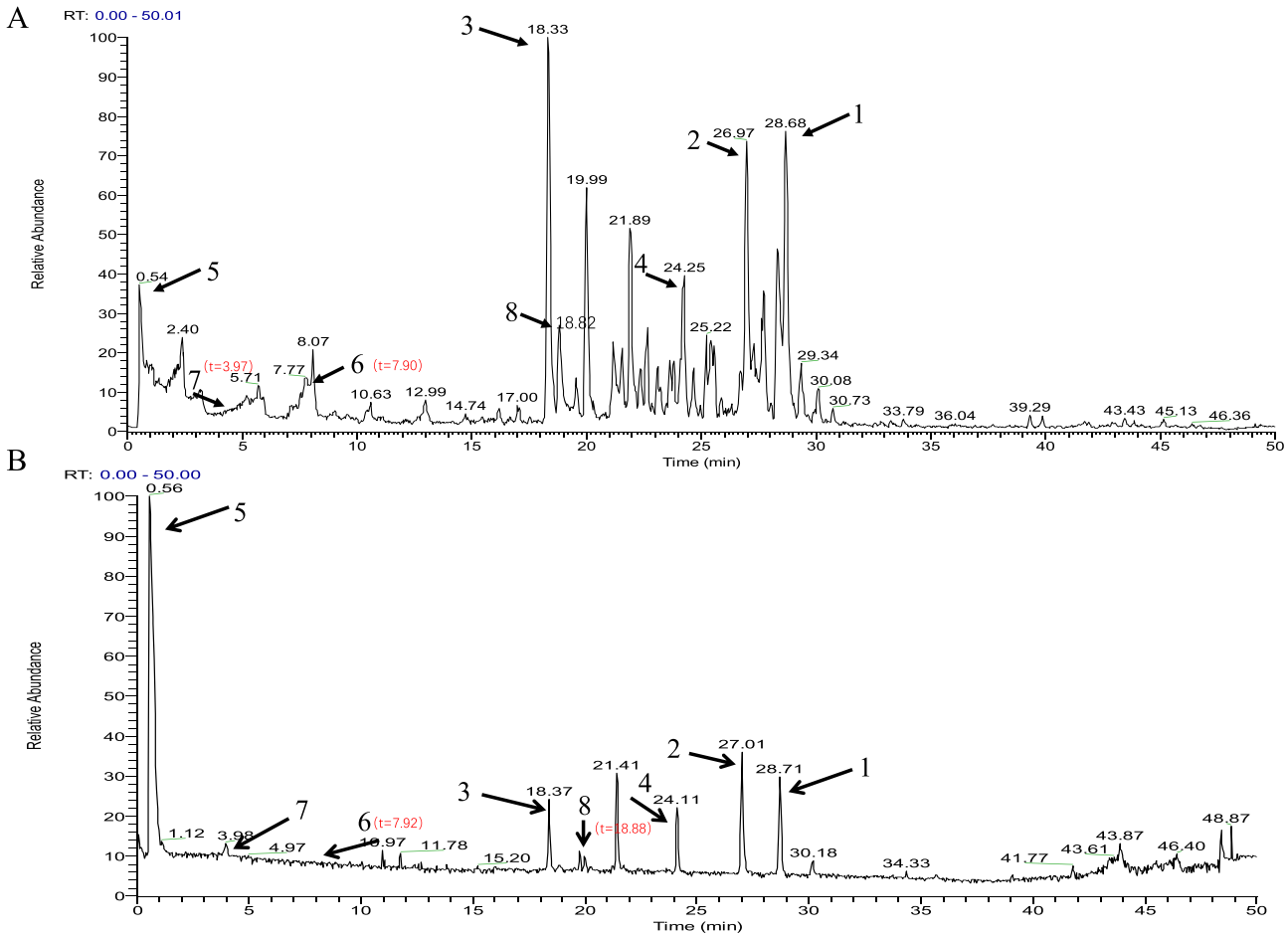

Figure 2 LC-MS analytical profiles. (**A**) Total ion flow chromatogram of SM; (**B**) total ion flow chromatogram of mixed standards; 1. schisandrin B; 2. schisandrin A; 3. schisandrol A; 4. schisantherin A; 5. betaine; 6. ferulic acid; 7. tetramethylpyrazine; 8. senkyunolide A. t means peak time in min.

ingredients, respectively, and then 1073 active targets were identified after de-duplication (see Figure 3 for the SM active ingredients-targets network).

Finding Common Gene Targets for SM and DKD

We obtained 253, 437 and 566 disease targets from the OMIM, Genecards and Disgenet databases, respectively. After taking and removing duplicate values, a total of 790 known targets of DKD were obtained. The potential targets of SM were mapped to the targets of DKD, and a total of 143 intersecting targets were available (Figure 4).

PPI Network Analysis

A total of 143 nodes and 2344 edges were obtained through the STRING online database platform (Figure 5A), which were imported into Cytoscape 3.8.2, and then the topological parameters (degree, betweenness and closeness) of all nodes in the network were analyzed by the Centiscape plug-in, resulting in a core network consisting of 25 nodes and 294 edges (Figure 5B). The top 20 relevant targets, which are potential core proteins for SM treatment of DKD, were filtered by degree values (Figure 5C).

GO and KEGG Analysis

GO and KEGG pathway enrichment analysis was performed using DAVID 5.6. The visualization process was completed using the bioinformatics website (http://www.bioinformatics.com.cn/). Figure 6A shows the results of enrichment processing for biological processes (BP), cellular components (CC), and molecular functions (MF) (TOP10). We

Table 2 Active Ingredients in SM Searched by LC/MS and Databases

Herb Name	Code Name	Molecule ID	Molecule Name	OB (%)	DL
Schisandrae chinensis fruit (Wuweizi, WWZ)	WWZ1	ID15560279	Calarene	52.16	0.11
	A1	ID92231	Spathulenol	82.33	0.12
	WWZ2	ID6450812	Beta-Gurjunene	51.36	0.1
	WWZ3	ID12311396	(+)-Alpha-Longipinene	57.47	0.12
	WWZ4	ID165536	Aristolone	45.31	0.13
	WWZ5	ID433636	Longikaurin A	47.72	0.53
	WWZ6	ID285342	Deoxyharringtonine	39.27	0.81
	A2	ID3026	Dibutyl Phthalate	64.54	0.13
	WWZ7	ID9845703	Citraurin beta	20.53	0.56
	WWZ8	ID98914	Arnebin 7	73.85	0.18
	WWZ9	ID12305213	(+)-aristolone	43.91	0.13
	WWZ10	ID91864462	Angeloylgomisin O	31.97	0.85
	WWZ11	ID5318785	Schizandrer B	30.71	0.83
	WWZ12	ID5497182	Clupanodonic acid	44.01	0.15
	WWZ13	ID3001662	Gomisin-A	30.69	0.78
	WWZ14	ID14992067	Gomisin G	32.68	0.83
	WWZ15	ID11495015	Gomisin R	34.84	0.86
	WWZ16	ID5318663	5,7-dihydroxy-2-(4-hydroxy-3-methoxyphenyl)-6-[(2S,3R,4S,5S,6R)-3,4,5-trihydroxy-6-(hydroxymethyl)oxan-2-yl]oxychromen-4-one	20.9	0.83
	WWZ17	ID443027	Wuweizisu C	46.27	0.84
	WWZ18	ID643733	Wyerone	79.24	0.13
	WWZ19	ID108130	Schisandrin B	-	-
	WWZ20	ID155256	Schisandrin A	-	-
	WWZ21	ID23915	Schisandrol A	-	-
	WWZ22	ID151529	Schisantherin A	-	-
	WWZ23	ID247	Betaine	-	-
Chuanxiong rhizoma (Chuanxiong, CX)	CX1	ID5282184	Mandenol	42	0.19
	CX2	ID161748	Myricanone	40.6	0.51
	CX3	ID160179	Perlolyrine	65.95	0.27
	CX4	ID91726743	Senkyunone	47.66	0.24
	CX5	ID10873344	Wallichilide	42.31	0.71
	CX6	ID12303645	Sitosterol	36.91	0.75
	CX7	ID6037	Taurocyamine	68.96	0.71
	CX8	ID14296	Tetramethylpyrazine	20.01	0.03
	CX9	ID5284421	Methyl Linoleate	41.93	0.17
	CX10	ID91457	Beta-Eudesmol	21.09	0.10
	A2	ID3026	Dibutyl Phthalate	64.64	0.13
	A1	ID13854252	Spathulenol	53.04	0.12
	CX11	ID10208	Chrysophanol	18.64	0.21
	CX12	ID335	O-Cresol	62.45	0.02
	CX13	ID445354	Retinol	19.53	0.16
	CX14	ID6989	Thymol	41.47	0.03
	CX15	ID7127	Methyl Eugenol	73.36	0.04
	CX16	ID8181	Methyl Palmitate	18.09	0.12
	CX17	ID12315453	Neocnidilide	83.83	0.07
	CX18	ID160710	Cnidilide	77.55	0.07
	CX19	ID689043	Caffeicacid	25.76	0.05
	CX20	ID68776935	Senkyunolide B	43.18	0.08

(*Continued*)

Table 2 (Continued).

Herb Name	Code Name	Molecule ID	Molecule Name	OB (%)	DL
	CX21	ID445858	Ferulic acid	39.56	0.06
	CX22	ID3085257	Senkyunolide A	26.56	0.07
Oyster shell	ML1	ID24498	Calcium Sulphate	-	-
(Muli, ML)	ML2	ID5359268	Aluminum	-	-
	ML3	ID24456	Calcium Phosphate	-	-
	ML4	ID5461123	Silicon	-	-
	ML5	ID10112	Calcium Carbonate	-	-
	ML6	ID4068592	Taurine	24.37	0.01

found that the top three BPs were positive regulation of gene expression, negative regulation of gene expression and negative regulation of apoptotic process, respectively; the top three CCs were extracellular region, extracellular space and macromolecular complex, respectively; the top three MFs were enzyme binding, protein binding and identical protein binding, respectively. KEGG enrichment analysis screened out 174 signaling pathways, which were mainly enriched in the AGE-RAGE signaling pathway in diabetic complications. Based on the degree of enrichment, we selected the top 20 ranked signaling pathways for bubble plot display (Figure 6B).

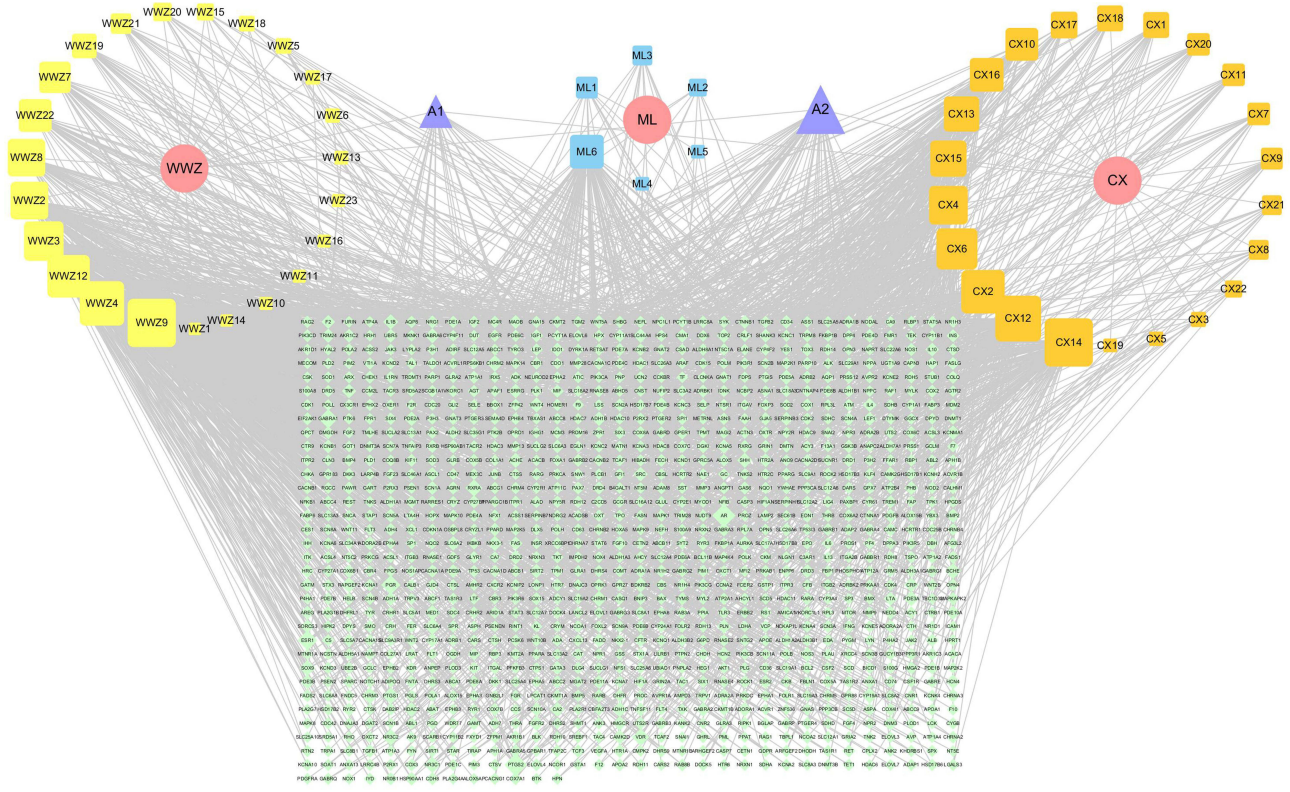

Figure 3 SM active ingredients-target network. Red represents the 3 herbs in SM; bright yellow, orange and blue represent the active chemical ingredients in WWZ, CX and ML, respectively, and purple represents the common active chemical ingredients in WWZ and CX; green represents the gene targets directly related to these components; the degree of association is indicated by the shape size of the nodes; the larger the association, the larger the nodes.

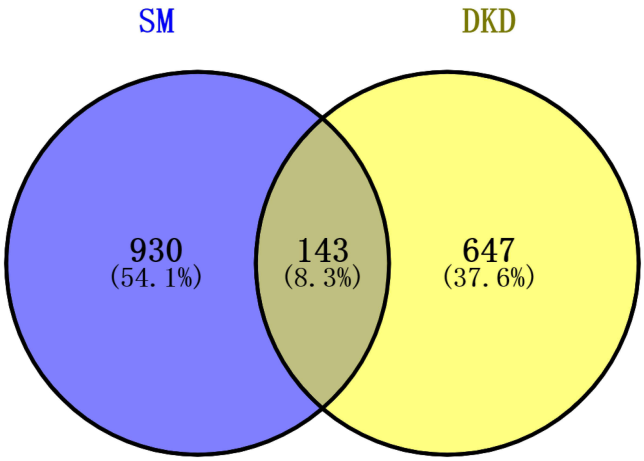

Figure 4 Venn diagram of potential targets of SM-DKD. Obtained through the Venn 2.1.0 platform. Purple represents potential targets where SM acts and yellow represents targets involved in DKD.

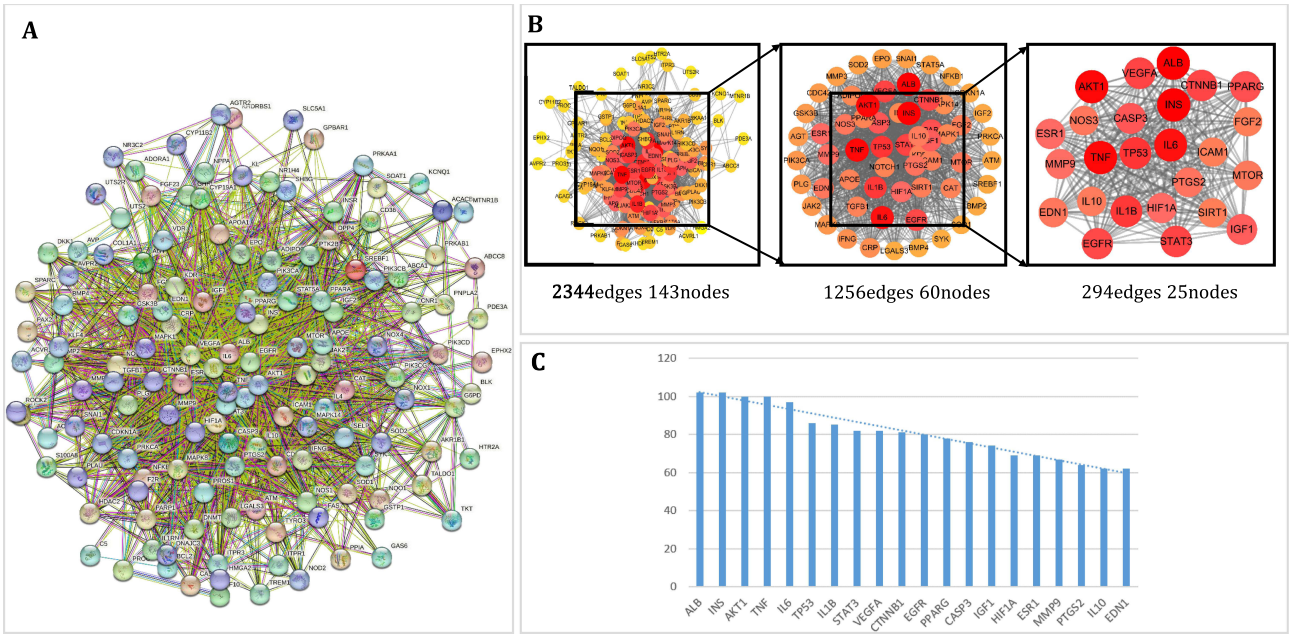

Figure 5 (**A**) Preliminary PPI map of SM-DKD displayed on STRING online website; (**B**) final core PPI map after 2 screening of preliminary PPI by analyzing degree, betweenness and closeness with applied Cytoscape software; (**C**) key targets (top 20) vertical axis indicates degree, horizontal axis indicates gene name.

Chemical Composition-Potential Target-Pathway Network Construction

To further determine the mechanism of action of SM on DKD, we integrated the complete pharmacological network based on all involved ingredients, key targets screened by PPI and their corresponding important signaling pathways. Based on the comprehensive screening of parameters, we visualized the relationship between the top 20 pathways and chemical components of KEGG ranking using Cytoscape to clearly demonstrate the pathways of action of the active chemical ingredients of SM on DKD (Figure 7).

Molecular Docking Verification

The most important component of SM was analyzed by chemical composition-potential target-pathway network is (+)-aristolone, representing it plays a crucial role in SM against DKD. To verify the degree of binding between this component and our core target, we used (+)-aristolone as a ligand and TNF-α, IL-6, IL-1β, IL-10, and AGEs as

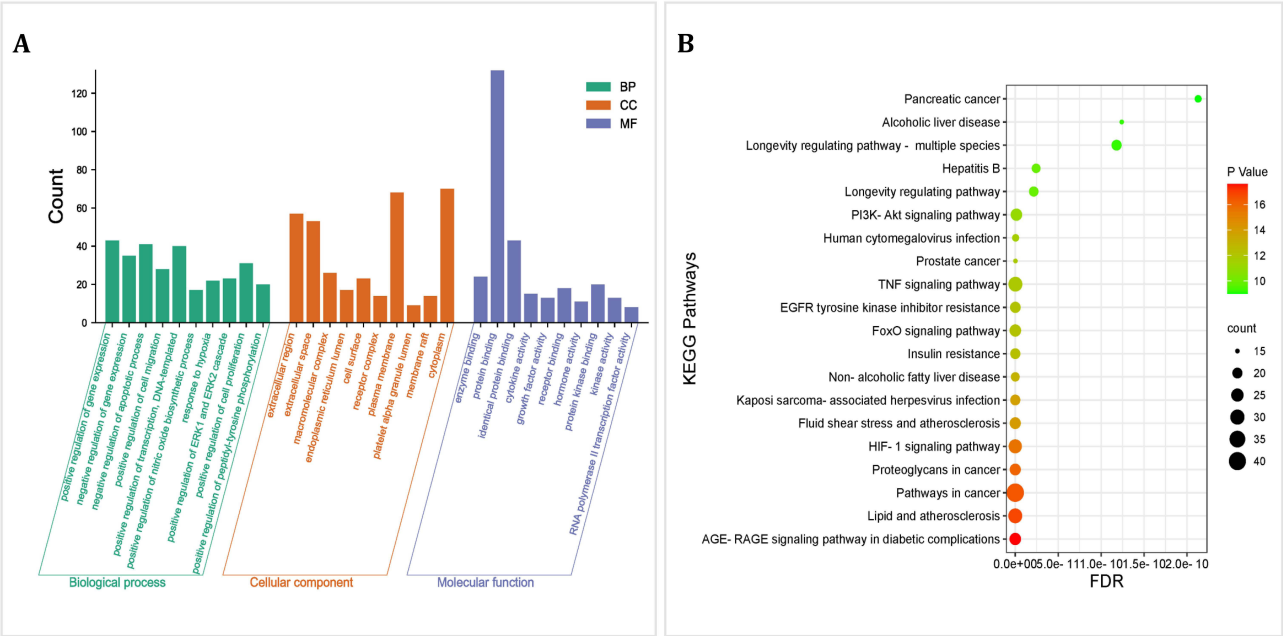

Figure 6 KEGG and GO enrichment graphs. (**A**) Green represents BP, orange represents CC, purple represents MF, and the height of the bar represents the number of enrichment; (**B**) the size of the bubble represents the number of gene enrichment, the larger the bubble, the more the number of genes; the darker the color, the smaller the P value, the greater the significance of enrichment.

receptors. Lower values of binding energy indicate more stable binding between the receptor and ligand. A cut-off of −5.0 kcal/mol is usually used.[37,38] The 2D chemical structure of the key component (+)-aristolone is shown in Figure 8A; the binding interaction of (+)-aristolone with the core target is shown in Figure 8B; the panoramic and local landscape of the receptor–ligand interaction is shown in Figure 8C.

Effect of SM on Water Intake and Food Consumption in DKD Rats

The DKD rat model was constructed by HSHF+STZ, and the results of the network pharmacology analysis were verified. At week 12, water consumption and food intake were significantly increased in DKD rats compared to the control group ($P < 0.01$). Administration of different doses of SM improved these symptoms to different degrees (Figure 9A and B).

Effect of SM on Blood Glucose, 24hUTP, Creatinine and BUN in DKD Rats

Compared with the control group, blood glucose, 24hUTP, serum creatinine and BUN were significantly increased in DKD rats ($P < 0.01$). SM effectively reduced 24hUTP, serum creatinine and BUN in DKD rats in all dose groups ($P < 0.01$). In addition, SM lowered the blood glucose level of DKD rats to some extent, although the difference in results was not statistically significant ($P > 0.05$) (Figure 10A-D). These above findings suggest that SM improved renal function in DKD rats.

SM Ameliorates Pathological Damage in DKD Rats

In the present study, HE, PASM and MASSON staining observations showed glomerular hypertrophy, mesangial cell proliferation, mesangial matrix expansion, glomerular basement membrane thickening, tubular lumen expansion and interstitial inflammatory cell infiltration in DKD rats. TEM showed homogeneous thickening of glomerular basement membrane, increased mesangial matrix and extensive fusion or disappearance of foot process. Compared with the DKD group, renal injury was improved to varying degrees in all SM dose groups and the effect was more pronounced with increasing dose. The histopathological results showed that SM improved the renal pathological injury and inflammatory

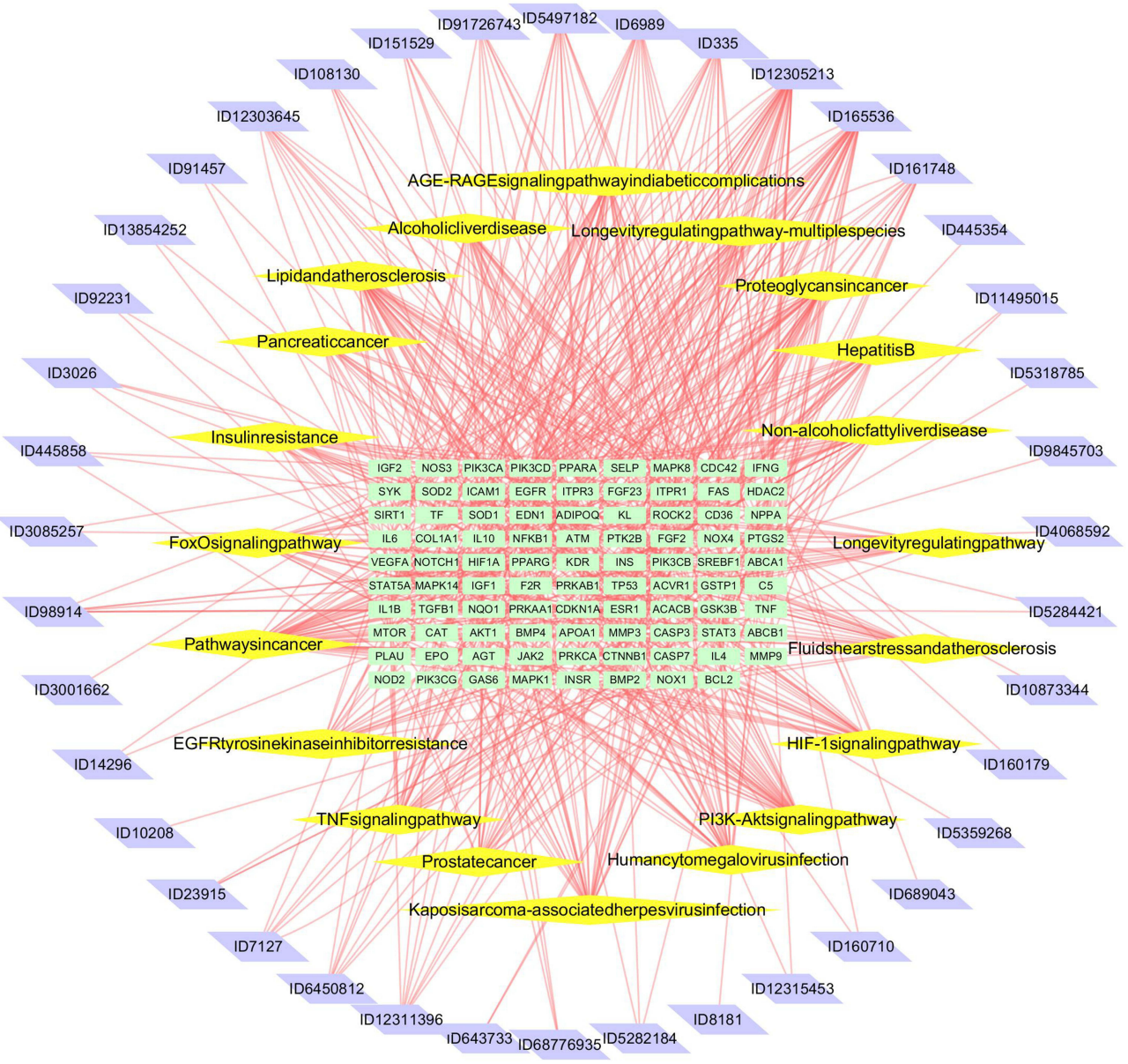

Figure 7 Chemical composition-potential target-pathway network diagram of SM for DKD treatment. Green represents potential gene targets, purple represents the active ingredients of SM, yellow represents the most significant signaling pathways, and red lines represent their interactions.

response in DKD rats (Figure 11). All of these results indicated that the high dose was the most effective for DKD among the three different doses. Therefore, we selected the SM-H group for further mechanistic studies.

SM Regulates AGEs-RAGE Signaling Pathway in DKD Rats

To further explore the potential mechanisms of SM, combined with the results of network pharmacology demonstration, the top ranked potential mechanism of SM for DKD is AGEs-RAGE signaling pathway in diabetic complications; also, several important inflammatory factors are on the top 30 core network. It is well known that although comprehensive mechanisms reveal the progression of DKD, the most convincing evidence emphasizes the importance of hyperglycemia-related formation of advanced glycosylation end products (AGEs) in DKD. Therefore, the AGEs-RAGE signaling pathway was selected as the main inflammation-related signaling pathway for experimental validation. The expression levels of AGEs and RAGE were significantly higher in DKD rats

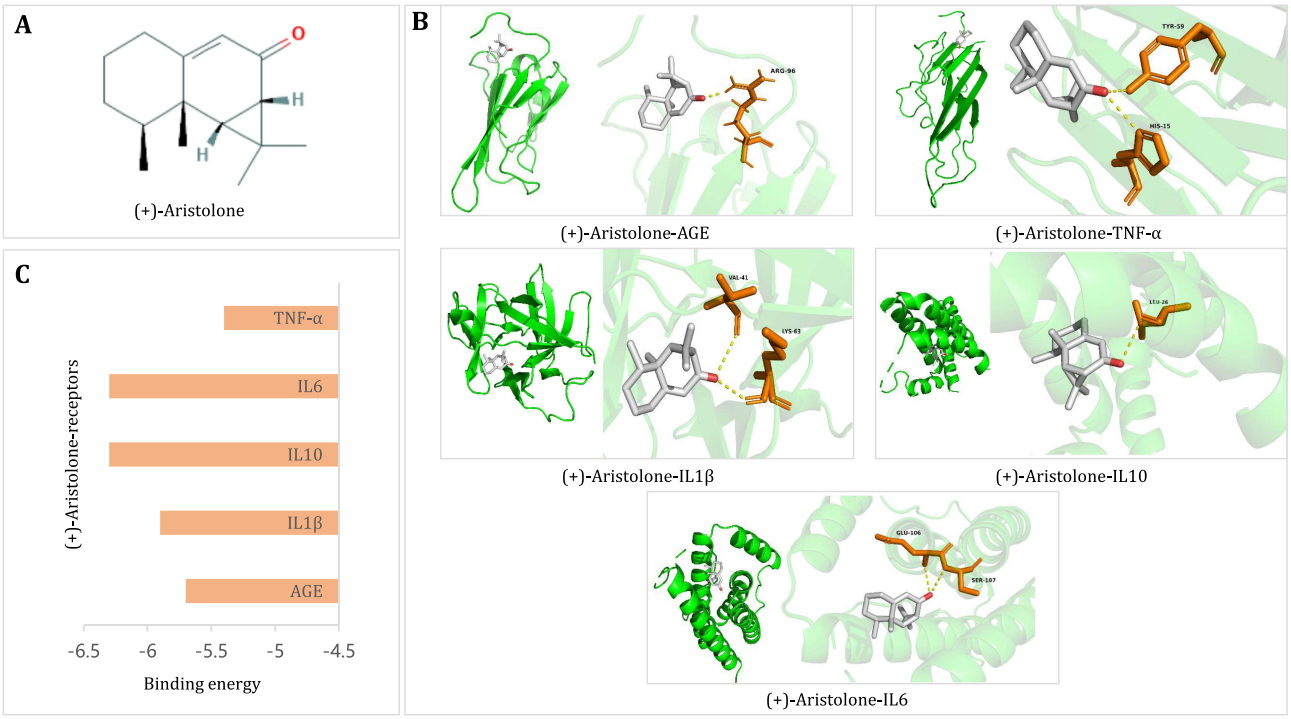

Figure 8 Molecular docking results are demonstrated. (**A**) 2D chemical structure of the key component (+)-aristolone; (**B**) binding energy bars of (+)-aristolone with AGE, TNF-α, IL1β, IL10 and IL6, respectively; (**C**) overall and local landscape of (+)-aristolone interactions with AGE, TNF-α, IL1β, IL10, and IL6, respectively.

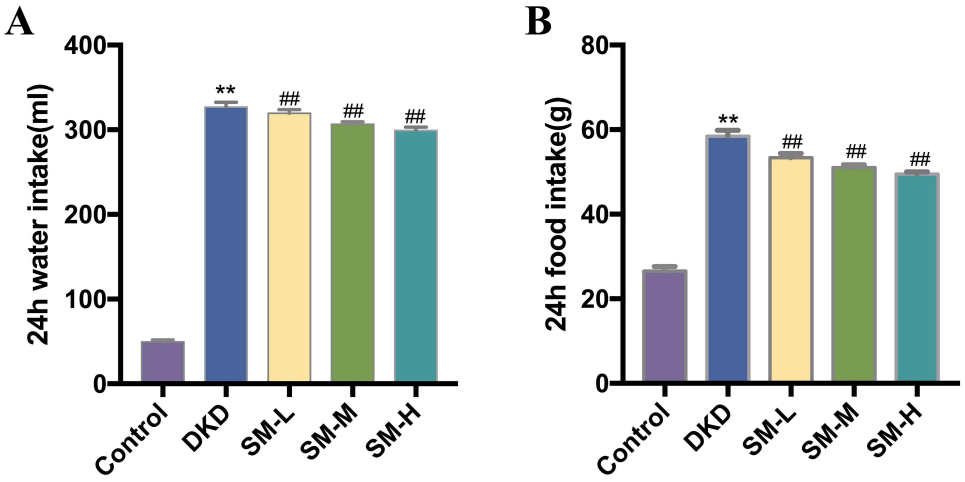

Figure 9 SM improved the general symptoms of DKD rats. (**A**) Water intake of rats at the end of the experiment; (**B**) food intake of rats at the end of the experiment. Data are expressed as mean±SD (n = 6). ** P < 0.01, compared with the control group; ## P < 0.01, compared with the DKD group.

compared to control rats (P < 0.01). In addition, the levels of AGEs and RAGE were significantly lower in the SM group compared to DKD rats (P < 0.01) (Figure 12).

Effect of SM on the Expression of Inflammatory Factors in the Renal Tissue of DKD Rats

Based on the results of PPI analysis to screen the core genes, we selected inflammatory cytokines including IL-1β, IL-6, IL-10 and TNF-α for experimental validation. Compared with the control group, the levels of inflammatory cytokines IL-1β, IL-6 and TNF-α were significantly increased and the level of IL-10 was decreased (P < 0.01) in the DKD group. SM treatment effectively upregulated IL-10 levels and downregulated IL-1β, IL-6, and TNF-α levels (P < 0.01) (Figure 13).

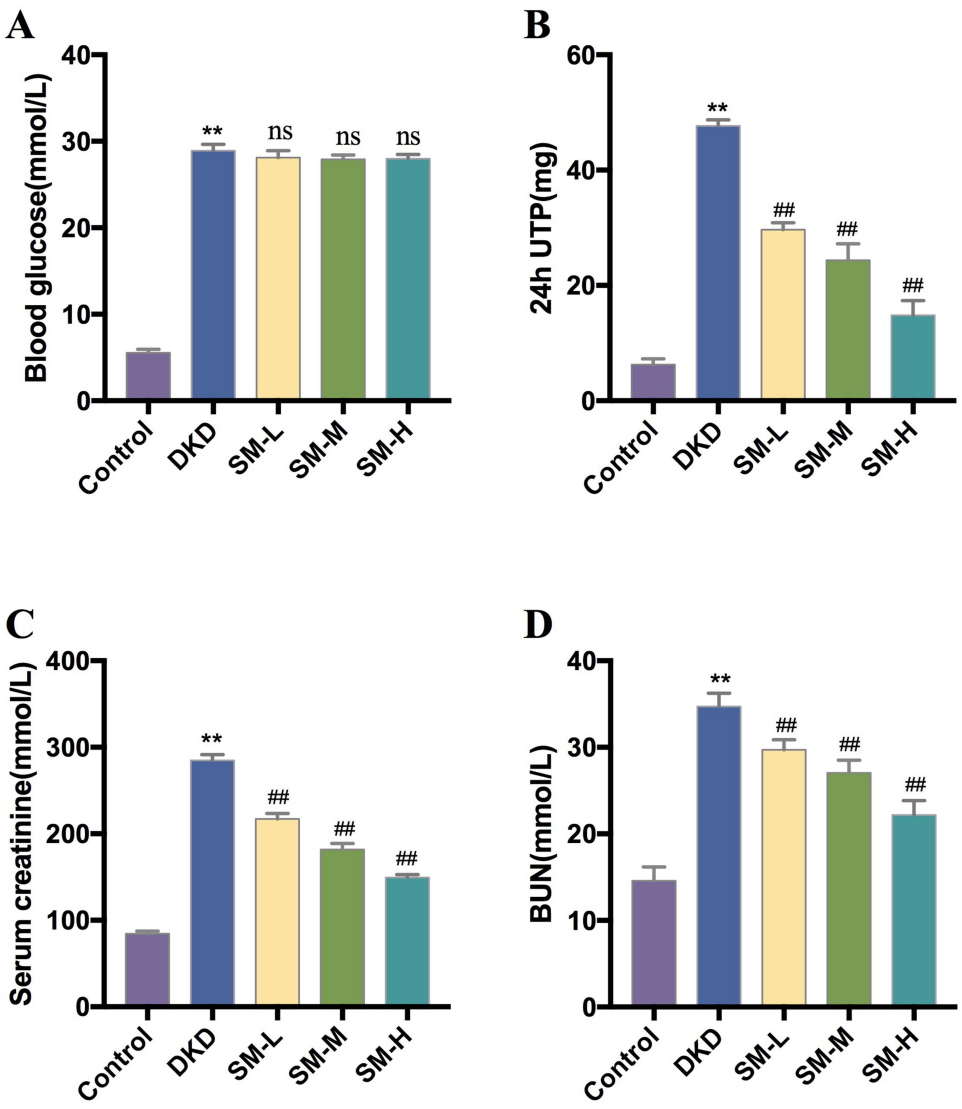

Figure 10 SM improved the indicators of renal injury in DKD rats. (**A**) Blood glucose level at the end of the experiment; (**B**) 24hUTP at the end of the experiment; (**C**) creatinine level at the end of the experiment. (**D**) BUN level at the end of the experiment. Data are expressed as mean ± SD (n = 6). ** P < 0.01, compared with the control group; ## P < 0.01, compared with the DKD group. ns, not significant.

Discussion

This study revealed for the first time that SM may improve renal inflammatory response through modulating AGEs-RAGE signaling pathway for the treatment of DKD, and this result provides a scientific basis for clinical application and creates a new direction for exploring the application of SM.

We screened 53 chemical components of SM with strong bioactivity and oral availability by means of comprehensive data mining and LC-MS, but finally, after analysis, only 40 components were found to play an effective role in the treatment of DKD by SM, and the most important of these components was (+)-aristolone. The molecular docking results also showed good binding between (+)-aristolone and the core target, indicating that it not only has good gastrointestinal absorption properties in SM but also binds well to the DKD core target. In fact, there are no reports of direct intervention with aristolone in DKD, but the potential of aristolone in the treatment of DKD can be found based on other relevant reports. Sulyman et al[39] used phytochemical analysis techniques to qualitatively and quantitatively analyze the chemical composition of the ethanolic (REAR) extract of Aristolochia roots, showing that the majority of the extract consisted of aristolone (92.3%). After 11 days of oral treatment of STZ-induced diabetic rats with REAR extract, blood glucose was

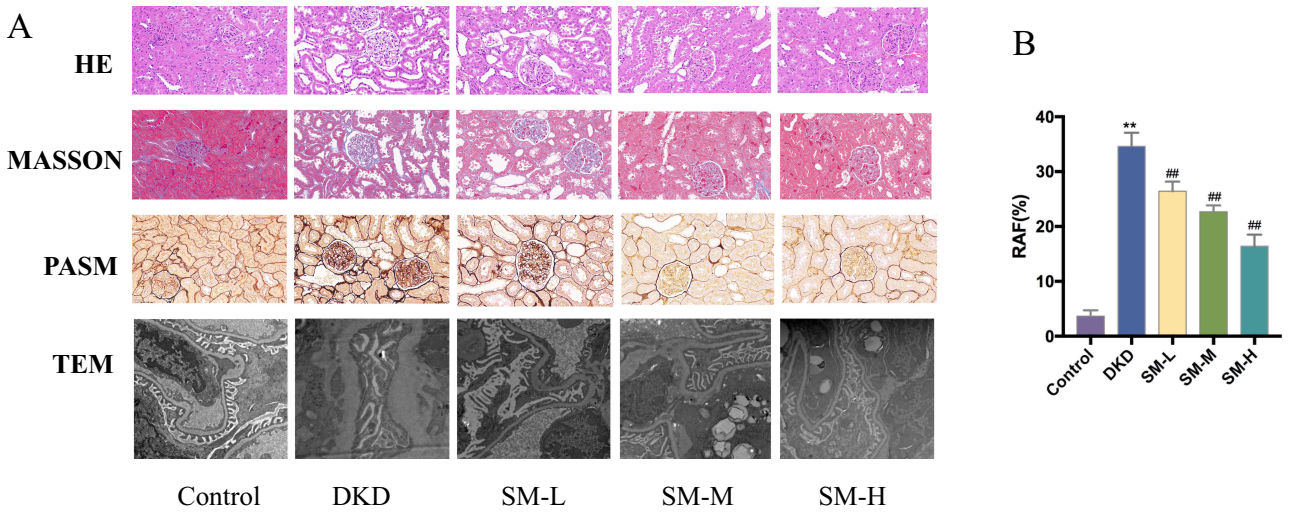

Figure 11 (**A**) SM ameliorated renal pathological damage in DKD rats. Light microscopy (HE, MASSON and PASM staining, 400×) and TEM (15,000×) of kidney tissues from DKD rats; (**B**) relative area fibrosis quantification(RAF) by MASSON.** P < 0.01, compared with the control group; ## P < 0.01, compared with the DKD group.

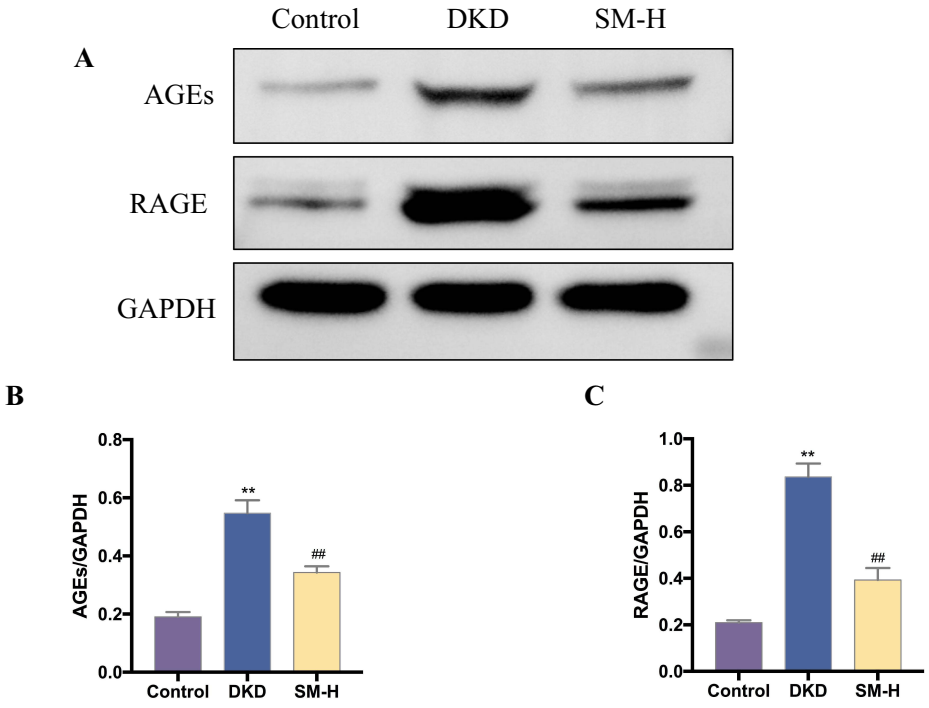

Figure 12 SM inhibits AGEs-RAGE pathway in DKD rats. (**A**) Representative bands of AGEs and RAGE proteins detected by Western blot. (**B**) Relative protein levels of AGEs in each group of rats; (**C**) relative protein levels of RAGE in each group of rats. Data are expressed as mean ± SD (n = 3). ** P < 0.01, compared with the normal group; ## P < 0.01, compared with the DKD group.

significantly reduced (>90%) to normal levels (≤120 mg/dl); GLY concentration and GPDH activity were significantly increased in the liver of diabetic rats treated with REAR extract compared to the untreated diabetic group, indicating the antidiabetic potential of aristolone. Fang et al found that aristolone could activate the PDK1-Akt-eNOS-NO relaxation pathway and stimulate the opening of K channels in an herb named *Nardostachys jatamansi DC*, which could exert anti-hypertensive effects, which may indirectly shed some light on the treatment of DKD;[40] furthermore, in an in vitro bioassay, (+)-aristolone exhibited promising anti-inflammatory activity by inhibiting the release of TNF-α in RAW 264.7 macrophages.[41] In addition, thymol, clupanodonic acid, sitosterol and other components occupy an important position in

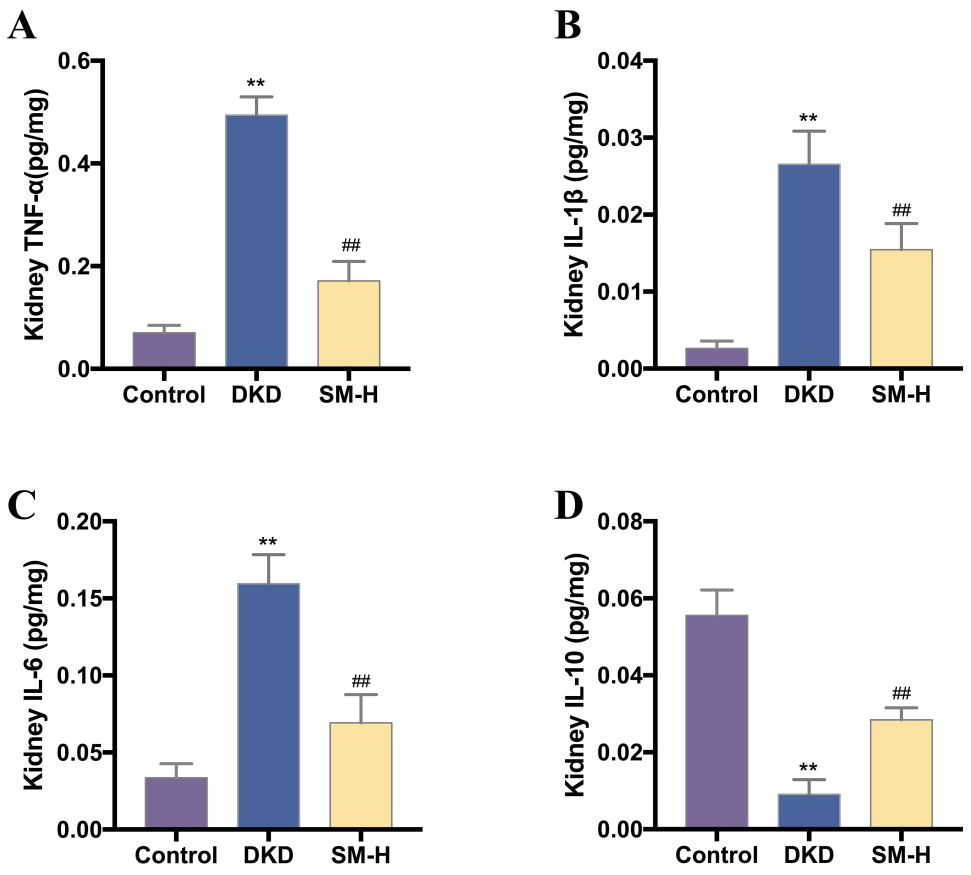

Figure 13 SM ameliorated the inflammatory response in DKD rats. (**A**) Levels of TNF-α in the kidney. (**B**) Levels of IL-1β in the kidney. (**C**) Levels of IL-6 in the kidney. (**D**) Levels of IL-10 in the kidney. Data are expressed as mean ± SD (n = 6). ** P < 0.01, compared with the control group; ## P < 0.01, compared with the DKD group.

the network. Unfortunately, the current reports have mostly investigated the effects of single active ingredients.[42–45] However, TCM is characterized by multiple components acting together. There are still no studies that have been able to elucidate how this cumulative effect arises. Therefore, in future studies, we will continue to investigate the underlying mechanisms of multiple components in network pharmacology working together to treat DKD.

Most notably, on the basis of KEGG pathway enrichment analysis, we found that the AGEs-RAGE signaling pathway is more closely associated with DKD pathogenesis compared to other pathways. There is no doubt that the increase of advanced glycosylation end products (AGEs) and the accumulation of their receptors (RAGE) due to hyperglycemia play a central role in the multiple pathogenesis of DKD.[46] AGEs are non-enzymatic glycosylation products formed by aldehyde or ketone groups of glucose or other reducing sugars with biological macromolecules such as proteins, lipids or nucleic acids through a series of dehydration, oxidation and rearrangement under non-enzymatic conditions.[47] AGEs can be synthesized in vivo or ingested through exogenous foods. RAGE is the most common receptor for AGEs and is more frequently expressed in the kidney. AGEs can mediate the development of DKD either directly or by binding to RAGE. The mechanisms include oxidative stress, miRNAs, cytokines, inflammatory responses and activation of the RAAS system, and their effects include podocytes, endothelial cells, and renal tubular epithelial cells in the mesangial nucleus.[48,49] It has been shown that RAGE overexpressing mice show increased urinary protein, decreased renal function, mesangial hyperplasia and glomerulosclerosis in the kidney.[50] The AGEs-RAGE axis induces renal oxidative stress and chronic inflammation through the activation of various signaling pathways, such as including phosphatidylinositol 3-kinase/protein kinase B/(PI3K/Akt), janus kinase-signal transducers and activators of transcription factor (JAK2/STAT), mitogen-activated protein kinase/extracellular signal-regulated kinase (MAPK/ERK), and Nox/ROS/NF-κB.[51–54] AGE-RAGE interaction induces NF-κB activation and oxidative stress through MAPK signaling pathway, which further stimulates the expression of pro-inflammatory cytokines.[55] AGEs play an important role in ROS-induced chronic inflammation. It has been shown that

AGEs mediate the expression of NOX4, an important source of ROS in the kidney, in a RAGE-dependent manner, and that excess ROS can allow NF-κB to enter the nucleus and cause multiple inflammatory cytokines (eg, IL-6, IL-1β, TNF-α, MCP-1) and adhesion molecules (eg, ICAM-1, VEGF, VCAM-1) expression and release, exacerbating the inflammatory response.[56] The increased NF-κB will in turn upregulate the expression of RAGE, forming a vicious circle, and silencing the RAGE gene can block the activation of NF-κB.[57] In addition to these signaling pathways, AGEs/RAGE can also activate NLPR3 inflammatory vesicles and induce inflammatory responses via endoplasmic reticulum stress.[58,59]

The inflammatory response has been shown to be an important inducer and facilitator in the pathogenesis of DKD. However, damage to the kidney by chronic inflammation underlies the structural changes in DKD function. There is growing evidence of a relationship between inflammation and fibrosis, and that fibrosis may be the end result of persistent inflammation.[60] TNF-α is a cytokine with significant pro-inflammatory effects, mainly produced by monocytes and macrophages, but also synthesized and secreted in glomerular mesangial cells, endothelial cells and epithelial cells.[61] In DKD, TNF-α and its receptors TNFR1 and TNFR2 are involved in the synthesis of fibrogenic factors, chemokines, growth factors, and extracellular matrix proteins, which amplify the cascade effects of inflammation and mediate inflammatory effects on a variety of renal intrinsic cells.[62] Elevated serum and urinary TNF-α levels have been reported in patients with DKD and are closely associated with proteinuria in diabetic patients.[63] TNF-α can alter glomerular basement membrane permeability and participate in apoptosis and necrosis in DKD patients and can also reduce glomerular filtration rate by affecting renal hemodynamics.[64] Studies have shown that soluble TNF-α antagonists can attenuate DKD-related renal injury.[65] IL-6 plays a key role in the chronic inflammatory environment of DKD and is able to maintain the stability of the renal environment. Elevated IL-6 has been found in the urine and kidneys of patients with DKD, which is associated with renal hypertrophy and urinary protein excretion.[66] Neutrophil infiltration, renal hypertrophy, and podocyte hypertrophy have been closely associated with IL-6.[67] Tocilizumab, a humanized antibody that blocks the IL-6 receptor (IL-6R), has been reported to reduce inflammation and oxidative stress to improve pathological changes in DKD rats.[68] IL-1β can stimulate glomerular mesangial cell proliferation and induce inflammatory mediators such as IL-6, TNF-α, prostaglandins, and gamma interferon through autocrine or paracrine forms and is thought to be closely associated with the development of diabetes and its microangiopathy.[69] In addition, IL-1β also causes abnormal changes in endothelial cell permeability by promoting the production and release of prostaglandin E and phospholipase A2, thus affecting glomerular microvascular dynamics and ultimately leading to the formation of renal fibrosis.[70] IL-1β induces proliferation of mesangial cells and promotes TGF-β expression, causing glomerular hypertrophy and tubulointerstitial fibrosis.[71] A clinical trial in patients with type 2 diabetes showed that IL-1β receptor antagonists improved glycemia and reduced markers of systemic inflammation in patients.[72] IL-10 is a potent anti-inflammatory cytokine that inhibits most pro-inflammatory cytokines and is secreted by M2-type macrophages. IL-10 antagonizes the effects of TNF-α via the p38/MAPK pathway.[73] In addition, IL-10 also activates HO-1 to inhibit iNOS activity.[74]

The innovation of this study is obvious. First, this study is the first to use multiple analytical tools to discover the important role of AGEs/RAGE pathways and inflammatory responses in DKD, and thus it is a more comprehensive study. Secondly, several databases were selected for herbal composition mining to complete a comprehensive and rigorous pre-screening work in this study. However, there are still some shortcomings in this study. On the one hand, network pharmacology is a still developing discipline and can only be used for those targets that have been discovered, not for the discovery of new ones. On the other hand, many monomer components in SM still need to be verified by in vivo and in vitro experiments.

Above, in this study, we comprehensively analyzed the potential of SM for the treatment of DKD through network pharmacology and found that the inflammatory response associated with AGEs/RAGE pathway may be the core mechanism of DKD development. We then tested this conjecture through in vivo experiments and found that SM could indeed effectively modulate the AGEs/RAGE pathway and thus improve the inflammatory response in DKD. Meanwhile, the molecular docking results showed stable binding of major SM components to pathway and target proteins, further demonstrating the feasibility of SM for the treatment of DKD. These findings provide an initial scientific basis for mechanistic studies of SM for DKD, offer hope for herbal-based complementary and alternative therapies, and offer the possibility of combining emerging methodologies with traditional theories.

Data Sharing Statement

The original data involved in this study can be requested by contacting the corresponding author (MZ) or the first author (HL or AD).

Ethics Statement

The in vivo experiments involved in this study were partially reviewed and approved by the Animal Ethics Committee of Beijing University of Chinese Medicine.

Author Contributions

All authors made a significant contribution to the work reported, whether that is in the conception, study design, execution, acquisition of data, analysis and interpretation, or in all these areas; took part in drafting, revising or critically reviewing the article; gave final approval of the version to be published; have agreed on the journal to which the article has been submitted; and agree to be accountable for all aspects of the work.

Funding

This work was supported by National Natural Science Foundation of China (No. 82074242).

Disclosure

All authors report no conflicts of interest in this work.

References

1. Hou J, Haas M. Temporal Trends in the Epidemiology of Biopsy-Proven Glomerular Diseases: an Alarming Increase in Diabetic Glomerulosclerosis. *Clin J Am Soc Nephrol*. 2017;12(4):556–558. doi:10.2215/CJN.02190217
2. Sun H, Saeedi P, Karuranga S, et al. IDF Diabetes Atlas: global, regional and country-level diabetes prevalence estimates for 2021 and projections for 2045. *Diabetes Res Clin Pract*. 2022;183:109119.
3. Umanath K, Lewis JB. Update on Diabetic Nephropathy: core Curriculum 2018. *Am J Kidney Dis*. 2018;71(6):884–895.
4. American Diabetes Association. 6. Glycemic Targets: standards of Medical Care in Diabetes-2018. *Diabetes Care*. 2018;41(Suppl1):S55–S64.
5. Jia W, Weng J, Zhu D, et al. Standards of medical care for type 2 diabetes in China 2019. *Diabetes Metab Res Rev*. 2019;35(6):e3158.
6. Li S, Zhang B. Traditional Chinese medicine network pharmacology: theory, methodology and application. *Chin J Nat Med*. 2013;11(2):110–120.
7. National Kidney Foundation. KDOQI clinical practice guideline for diabetes and CKD: 2012 update. *Am J Kidney Dis*. 2012;60(5):850–886.
8. Huang Y, Lu W, Lu H. The clinical efficacy and safety of dapagliflozin in patients with diabetic nephropathy. *Diabetol Metab Syndr*. 2022;14(1):47.
9. Abegaz TM, Diaby V, Sherbeny F, Ali AA. Cost Effectiveness of Dapagliflozin Added to Standard of Care for the Management of Diabetic Nephropathy in the USA. *Clin Drug Investig*. 2022;42(6):501–511.
10. Alicic RZ, Johnson EJ, Tuttle KR. SGLT2 Inhibition for the Prevention and Treatment of Diabetic Kidney Disease: a Review. *Am J Kidney Dis*. 2018;72(2):267–277. doi:10.1053/j.ajkd.2018.03.022
11. Pecoits-Filho R, Perkovic V. Are SGLT2 Inhibitors Ready for Prime Time for CKD? *Clin J Am Soc Nephrol*. 2018;13(2):318–320. doi:10.2215/CJN.07680717
12. Wu T, Yang X, Cong Y, et al. Effects of Qidantang Granule on early stage of diabetic kidney disease in rats. *Aging*. 2022;14(11):4888–4896. doi:10.18632/aging.204121
13. Zhao J, Ai J, Mo C, Shi W, Meng L. Comparative efficacy of seven Chinese patent medicines for early diabetic kidney disease: a Bayesian network meta-analysis. *Complement Ther Med*. 2022;67:102831.
14. Liu J, Gao LD, Fu B, et al. Efficacy and safety of Zicuiyin decoction on diabetic kidney disease: a multicenter, randomized controlled trial. *Phytomedicine*. 2022;100:154079.
15. Li H, Dong S, Liu Y, et al. Efficacy and Safety of "Bushen Huoxue Therapy"-Based Combined Chinese and Western Medicine Treatment for Diabetic Kidney Disease: an Updated Meta-Analysis of 2105 Patients. *Evid Based Complement Alternat Med*. 2022;2022:3710074.
16. Zhang M, Liu M, Xiong M, Gong J, Tan X. Schisandra chinensis fruit extract attenuates albuminuria and protects podocyte integrity in a mouse model of streptozotocin-induced diabetic nephropathy. *J Ethnopharmacol*. 2012;141(1):111–118.
17. Ma Y, Deng Y, Li N, et al. Network pharmacology analysis combined with experimental validation to explore the therapeutic mechanism of Schisandra Chinensis Mixture on diabetic nephropathy. *J Ethnopharmacol*. 2023;302(Pt A):115768.
18. Hopkins AL. Network pharmacology: the next paradigm in drug discovery. *Nat Chem Biol*. 2008;4(11):682–690.
19. Wang X, Wang ZY, Zheng JH, Li S. TCM network pharmacology: a new trend towards combining computational, experimental and clinical approaches. *Chin J Nat Med*. 2021;19(1):1–11.
20. Liu J, Liu J, Tong X, et al. Network Pharmacology Prediction and Molecular Docking-Based Strategy to Discover the Potential Pharmacological Mechanism of Huai Hua San Against Ulcerative Colitis. *Drug Des Devel Ther*. 2021;15:3255–3276.
21. Ru J, Li P, Wang J, et al. TCMSP: a database of systems pharmacology for drug discovery from herbal medicines. *J Cheminform*. 2014;6:13.
22. Xue R, Fang Z, Zhang M, Yi Z, Wen C, Shi T. TCMID: traditional Chinese Medicine integrative database for herb molecular mechanism analysis. *Nucleic Acids Res*. 2013;41(Databaseissue):D1089–95.
23. Xu HY, Zhang YQ, Liu ZM, et al. ETCM: an encyclopaedia of traditional Chinese medicine. *Nucleic Acids Res*. 2019;47(D1):D976–D982.

24. Liu Z, Guo F, Wang Y, et al. BATMAN-TCM: a Bioinformatics Analysis Tool for Molecular mechANism of Traditional Chinese Medicine. *Sci Rep*. 2016;6:21146.
25. Tao W, Xu X, Wang X, et al. Network pharmacology-based prediction of the active ingredients and potential targets of Chinese herbal Radix Curcumae formula for application to cardiovascular disease. *J Ethnopharmacol*. 2013;145(1):1–10.
26. Xu X, Zhang W, Huang C, et al. A novel chemometric method for the prediction of human oral bioavailability. *Int J Mol Sci*. 2012;13 (6):6964–6982.
27. Daina A, Michielin O, Zoete V. SwissADME: a free web tool to evaluate pharmacokinetics, drug-likeness and medicinal chemistry friendliness of small molecules. *Sci Rep*. 2017;7:42717.
28. Zou J, Gao P, Hao X, Xu H, Zhan P, Liu X. Recent progress in the structural modification and pharmacological activities of ligustrazine derivatives. *Eur J Med Chem*. 2018;147:150–162.
29. Kim N, Priefer R. Retinol binding protein 4 antagonists and protein synthesis inhibitors: potential for therapeutic development. *Eur J Med Chem*. 2021;226:113856.
30. Daina A, Michielin O, Zoete V. SwissTargetPrediction: updated data and new features for efficient prediction of protein targets of small molecules. *Nucleic Acids Res*. 2019;47(W1):W357–W364.
31. Chao CH, Hsu JL, Chen MF, et al. Anti-hypertensive effects of *Radix Rehmanniae* and its active ingredients. *Nat Prod Res*. 2020;34 (11):1547–1552.
32. Goodsell DS, Zardecki C, Di Costanzo L, et al. RCSB Protein Data Bank: enabling biomedical research and drug discovery. *Protein Sci*. 2020;29 (1):52–65.
33. Wang Y, Xiao J, Suzek TO, et al. PubChem's BioAssay Database. *Nucleic Acids Res*. 2012;40(Databaseissue):D400–12.
34. El-Hachem N, Haibe-Kains B, Khalil A, Kobeissy FH, Nemer G. AutoDock and AutoDockTools for Protein-Ligand Docking: beta-Site Amyloid Precursor Protein Cleaving Enzyme 1(BACE1) as a Case Study. *Methods Mol Biol*. 2017;1598:391–403.
35. Baugh EH, Lyskov S, Weitzner BD, Gray JJ. Real-time PyMOL visualization for Rosetta and PyRosetta. *PLoS One*. 2011;6(8):e21931.
36. Su X, Yu W, Liu A, et al. San-Huang-Yi-Shen Capsule Ameliorates Diabetic Nephropathy in Rats Through Modulating the Gut Microbiota and Overall Metabolism. *Front Pharmacol*. 2022;12:808867.
37. Li C, Du X, Liu Y, et al. A Systems Pharmacology Approach for Identifying the Multiple Mechanisms of Action for the Rougui-Fuzi Herb Pair in the Treatment of Cardiocerebral Vascular Diseases. *Evid Based Complement Alternat Med*. 2020;2020:5196302.
38. Li X, Tang H, Tang Q, Chen W. Decoding the Mechanism of Huanglian Jiedu Decoction in Treating Pneumonia Based on Network Pharmacology and Molecular Docking. *Front Cell Dev Biol*. 2021;9:638366.
39. Sulyman AO, Akolade JO, Sabiu SA, Aladodo RA, Muritala HF. Antidiabetic potentials of ethanolic extract of Aristolochia ringens (Vahl.) roots. *J Ethnopharmacol*. 2016;182:122–128.
40. Fang J, Li R, Zhang Y, et al. Aristolone in Nardostachys jatamansi DC. induces mesenteric vasodilation and ameliorates hypertension via activation of the K_{ATP} channel and PDK1-Akt-eNOS pathway. *Phytomedicine*. 2022;104:154257.
41. Shen SM, Yang Q, Zang Y, Li J, Liu X, Guo YW. Anti-inflammatory aromadendrane- and cadinane-type sesquiterpenoids from the South China Sea sponge *Acanthella cavernosa*. *Beilstein J Org Chem*. 2022;18:916–925.
42. Amara I, Timoumi R, Annabi E, Ben Othmène Y, Abid-Essefi S. The protective effects of thymol and carvacrol against di (2-ethylhexyl) phthalate-induced cytotoxicity in HEK-293 cells. *J Biochem Mol Toxicol*. 2022;36(8):e23092.
43. Bellahcen S, Mekhfi H, Ziyyat A, et al. Prevention of chemically induced diabetes mellitus in experimental animals by virgin argan oil. *Phytother Res*. 2012;26(2):180–185.
44. Hajleh MNA, Khleifat KM, Alqaraleh M, et al. Antioxidant and Antihyperglycemic Effects of *Ephedra foeminea* Aqueous Extract in Streptozotocin-Induced Diabetic Rats. *Nutrients*. 2022;14(11):2338.
45. Suresh Y, Das UN. Long-chain polyunsaturated fatty acids and chemically induced diabetes mellitus. Effect of omega-3 fatty acids. *Nutrition*. 2003;19(3):213–228.
46. Molitch ME, Adler AI, Flyvbjerg A, et al. Diabetic kidney disease: a clinical update from Kidney Disease: improving Global Outcomes. *Kidney Int*. 2015;87(1):20–30.
47. Perrone A, Giovino A, Benny J, Martinelli F. Advanced Glycation End Products (AGEs): biochemistry, Signaling, Analytical Methods, and Epigenetic Effects. *Oxid Med Cell Longev*. 2020;2020:3818196.
48. Kumar Pasupulati A, Chitra PS, Reddy GB. Advanced glycation end products mediated cellular and molecular events in the pathology of diabetic nephropathy. *Biomol Concepts*. 2016;7(5–6):293–309.
49. Sanajou D, Ghorbani Haghjo A, Argani H, Aslani S. AGE-RAGE axis blockade in diabetic nephropathy: current status and future directions. *Eur J Pharmacol*. 2018;833:158–164.
50. Yamamoto Y, Kato I, Doi T, et al. Development and prevention of advanced diabetic nephropathy in RAGE-overexpressing mice. *J Clin Invest*. 2001;108(2):261–268.
51. Chen YH, Chen ZW, Li HM, et al. AGE/RAGE-Induced EMP Release via the NOX-Derived ROS Pathway. *J Diabetes Res*. 2018;2018:6823058.
52. Wu XQ, Zhang DD, Wang YN, Tan YQ, Yu XY, Zhao YY. AGE/RAGE in diabetic kidney disease and ageing kidney. *Free Radic Biol Med*. 2021;171:260–271.
53. Fukami K, Taguchi K, Yamagishi S, Okuda S. Receptor for advanced glycation endproducts and progressive kidney disease. *Curr Opin Nephrol Hypertens*. 2015;24(1):54–60.
54. Hong JN, Li WW, Wang LL, et al. Jiangtang decoction ameliorate diabetic nephropathy through the regulation of PI3K/Akt-mediated NF-κB pathways in KK-Ay mice. *Chin Med*. 2017;12:13.
55. Sanz AB, Sanchez-Niño MD, Ramos AM, et al. NF-kappaB in renal inflammation. *J Am Soc Nephrol*. 2010;21(8):1254–1262.
56. Cepas V, Collino M, Mayo JC, Sainz RM. Redox Signaling and Advanced Glycation Endproducts (AGEs) in Diet-Related Diseases. *Antioxidants*. 2020;9(2):142.
57. Hong J, Wang X, Zhang N, Fu H, Li W. D-ribose induces nephropathy through RAGE-dependent NF-κB inflammation. *Arch Pharm Res*. 2018;41 (8):838–847.
58. Chen Y, Liu CP, Xu KF, et al. Effect of taurine-conjugated ursodeoxycholic acid on endoplasmic reticulum stress and apoptosis induced by advanced glycation end products in cultured mouse podocytes. *Am J Nephrol*. 2008;28(6):1014–1022.

59. Hong J, Li G, Zhang Q, Ritter J, Li W, Li PL. D-Ribose Induces Podocyte NLRP3 Inflammasome Activation and Glomerular Injury via AGEs/RAGE Pathway. *Front Cell Dev Biol*. 2019;7:259.
60. Goldszmid RS, Trinchieri G. The price of immunity. *Nat Immunol*. 2012;13(10):932–938.
61. Navarro JF, Mora-Fernández C. The role of TNF-alpha in diabetic nephropathy: pathogenic and therapeutic implications. *Cytokine Growth Factor Rev*. 2006;17(6):441–450.
62. Niewczas MA, Gohda T, Skupien J, et al. Circulating TNF receptors 1 and 2 predict ESRD in type 2 diabetes. *J Am Soc Nephrol*. 2012;23(3):507–515.
63. Moriwaki Y, Yamamoto T, Shibutani Y, et al. Elevated levels of interleukin-18 and tumor necrosis factor-alpha in serum of patients with type 2 diabetes mellitus: relationship with diabetic nephropathy. *Metabolism*. 2003;52(5):605–608.
64. Elmarakby AA, Sullivan JC. Relationship between oxidative stress and inflammatory cytokines in diabetic nephropathy. *Cardiovasc Ther*. 2012;30(1):49–59.
65. DiPetrillo K, Coutermarsh B, Gesek FA. Urinary tumor necrosis factor contributes to sodium retention and renal hypertrophy during diabetes. *Am J Physiol Renal Physiol*. 2003;284(1):F113–21.
66. Wolkow PP, Niewczas MA, Perkins B, et al. Association of urinary inflammatory markers and renal decline in microalbuminuric type 1 diabetics. *J Am Soc Nephrol*. 2008;19(4):789–797.
67. Rayego-Mateos S, Morgado-Pascual JL, Opazo-Ríos L, et al. Pathogenic Pathways and Therapeutic Approaches Targeting Inflammation in Diabetic Nephropathy. *Int J Mol Sci*. 2020;21(11):3798.
68. Abdelrahman AM, Al Suleimani Y, Shalaby A, Ashique M, Manoj P, Ali BH. Effect of tocilizumab, an interleukin-6 inhibitor, on early stage streptozotocin-induced diabetic nephropathy in rats. *Naunyn Schmiedebergs Arch Pharmacol*. 2019;392(8):1005–1013.
69. Buraczynska M, Ksiazek K, Wacinski P, Zaluska W. Interleukin-1β Gene (*IL1B*) Polymorphism and Risk of Developing Diabetic Nephropathy. *Immunol Invest*. 2019;48(6):577–584.
70. Pérez-Morales RE, Del Pino MD, Valdivielso JM, Ortiz A, Mora-Fernández C, Navarro-González JF. Inflammation in Diabetic Kidney Disease. *Nephron*. 2019;143(1):12–16.
71. Vesey DA, Cheung C, Cuttle L, Endre Z, Gobe G, Johnson DW. Interleukin-1beta stimulates human renal fibroblast proliferation and matrix protein production by means of a transforming growth factor-beta-dependent mechanism. *J Lab Clin Med*. 2002;140(5):342–350.
72. Larsen CM, Faulenbach M, Vaag A, et al. Interleukin-1-receptor antagonist in type 2 diabetes mellitus. *N Engl J Med*. 2007;356(15):1517–1526.
73. Kontoyiannis D, Kotlyarov A, Carballo E, et al. Interleukin-10 targets p38 MAPK to modulate ARE-dependent TNF mRNA translation and limit intestinal pathology. *EMBO J*. 2001;20(14):3760–3770.
74. Gobert AP, Verriere T, Asim M, et al. Heme oxygenase-1 dysregulates macrophage polarization and the immune response to Helicobacter pylori. *J Immunol*. 2014;193(6):3013–3022.